The first two equations are used to find λ_1 and λ_2. If Eq. (8c) is applied, then these two equations become

$$(I_1 + M \cdot R^2)\ddot{\beta} + M \cdot R \cdot a \cdot \dot{\beta}^2 + M \cdot R \cdot g \cdot \cos\beta + \lambda_1 + 2 \cdot M \cdot R \cdot a \cdot \dot{\beta} \cdot \dot{\lambda}_2 + M \cdot R \cdot a \cdot \ddot{\beta} \cdot \lambda_2 = 0 \quad (9a)$$

$$M(a^2 + k^2)\ddot{\beta} - M \cdot R \cdot a \cdot \dot{\beta}^2 + M \cdot a \cdot g \cdot \sin\beta - \lambda_1 + M(a^2 + k^2)\ddot{\lambda}_2 + M \cdot R \cdot a \cdot \ddot{\beta} \cdot \lambda_2 + M \cdot a \cdot g \cdot \cos\beta \cdot \lambda_2 = 0. \quad (9b)$$

λ_1 disappears after adding the last two equations, and the equation of motion of the entire system (the attached disk and plate) is obtained:

$$[I_1 + M(R^2 + a^2 + k^2)]\ddot{\beta} + M \cdot g(R \cdot \cos\beta + a \cdot \sin\beta) + M(a^2 + k^2)\ddot{\lambda}_2 + 2 \cdot M \cdot R \cdot a(\dot{\beta} \cdot \dot{\lambda}_2 + \ddot{\beta} \cdot \lambda_2) + M \cdot g \cdot a \cdot \cos\beta \cdot \lambda_2 = 0. \quad (10)$$

The first term in the last equation presents the inertial moment (of the entire system) about the point O (positive in the counterclockwise direction). The second term is the contribution of gravity to the moment about the same point. The last three terms represent the moment that is applied by the motor on disk Σ_1 (the control moment), M_e:

$$M_e = -M(a^2 + k^2)\ddot{\lambda}_2 - 2 \cdot M \cdot R \cdot a(\dot{\beta} \cdot \dot{\lambda}_2 + \ddot{\beta} \cdot \lambda_2) - M \cdot g \cdot a \cdot \cos\beta \cdot \lambda_2. \quad (11)$$

The fact that the new formulation of Lagrange method offers a unified approach to all kinds of constraints is shown again if one drops all the terms that include λ_2 and its derivatives in Eq. (10). This means that the condition of a pin-joint at A is dropped and instead a rigid joint is considered. Then Eq. (10) converges to the well-known equation of vibrations of the entire system about point O, under the influence of gravity (a physical pendulum).

Cabannes gives an analytic solution of Eq. (3). For the case where the initial conditions are $\beta = \beta_0 = 0$ and $\dot{\beta} = \dot{\beta}_0$, this solution is

$$\dot{\beta}^2 - \left(\dot{\beta}_0^2 - \frac{g}{R}\frac{m}{1 + m^2}\right)e^{m\beta} - \frac{mg}{R(1 + m^2)}(\cos\beta + m\sin\beta) = 0 \quad (12)$$

where

$$m = \frac{2Ra}{a^2 + k^2}. \quad (13)$$

In Fig. 2 results for the case

$$M = I_1 = R = a = k = \dot{\beta}_0 = 1; \quad \beta_0 = (\lambda_2)_0 = (\dot{\lambda}_2)_0 = 0$$

are presented. These results were obtained by direct numerical integration of Eqs. (3) and (10), while Eq. (9) was used to solve for λ_1. β, λ_1, and λ_2 exhibit a periodic behavior that is different for each unknown. In order to verify the accuracy of the numerical integration the values of $\dot{\beta}$ and β, at any moment, were substituted into the left side of Eq. (12) and the result divided by $\dot{\beta}^2$. The absolute value of this relative error (in percents) is also shown and indicates that the numerical integration is associated with relatively small errors.

4 Conclusions

Recently a new formulation of the Lagrange method was presented by Rosen and Edelstein. This formulation offers a unified approach of dealing with holonomic or nonholonomic constraints that is correct from a variational mathematical point of view for both kinds of constraints.

The use of the new formulation to solve problems of control constraints has been presented in this note. The advantages of the new formulation are the following:

(a) It is straightforward and easy to apply. Thus, the new formulation is suitable for a general purpose computer code.

(b) There is a unified approach to all the kinds of constraints, holonomic or nonholonomic.

(c) It is possible to deal with constraints that include accelerations and nonlinear expressions of the velocities.

(d) There is a clear direct physical interpretation of the constraints, similar to that offered by Newton's method.

References

Cabannes, H., 1968, *General Mechanics*, Blaisdell Publishing Co. translation from French by S. P. Sutera.

Levi-Civita, T., 1926, *Meccanica Razionale*, Vol. II, Bologna, Nicola Zanichelli, pp. 303–306.

Rosen, A., and Edelstein, E., 1997a, "Investigations of a New Formulation of the Lagrange Method for Constrained Dynamic Systems," ASME Journal of Applied Mechanics, Vol. 64, pp. 116–122.

Rosen, A., and Edelstein, E., 1997b, Reply to a discussion by Professor P. Hagedorn of the paper "Investigation of a New Formulation of the Lagrange Method for Constrained Dynamic Systems," ASME Journal of Applied Mechanics, Vol. 64, pp. 1025–1027.

Rosen, A., and Edelstein, E., 1998, "A New Examination of the Problem of Constrained Dynamics," *Proceedings of the 38th Israel Ann. Conf. on Aerospace Sciences*, Feb. 25–26, pp. 186–197.

Steady-State Deflection of a Circular Plate Rotating Near Its Critical Speed

Jen-San Chen[1]

The steady-state response of a disk spinning near its critical speed and under space-fixed time-invariant load is analyzed by using von Karman's nonlinear plate model. It is found that as the disk rotates beyond a modified critical speed there exist three steady-state deflections, among which only one is in the same direction as the applied load and is stable in the presence of space-fixed damping.

Introduction

Conventional linearized plate theory predicts that the steady-state deflection of a spinning disk under space-fixed time-invariant load approaches infinity as the rotation speed approaches the critical speed. This conclusion contradicts experimental result that shows the existence of finite steady-state deflection even at the critical speed (Tobias and Arnold, 1957). In order to capture the physical essence of critical speed resonance, Raman and Mote (1999) recently adopted von Karman's plate model (Nowinski, 1964) to study the nonlinear oscillations of a disk spinning near its critical speed and subject to rotating damping. Since their analysis is performed in a rotating frame, the forcing terms are time-dependent and averaging technique has to be used. In many spinning disk applications, however, the external damping is space-fixed, such as the damping in circular saw guides and disk drive

[1] Associate Professor, Department of Mechanical Engineering, National Taiwan University, Taipei Taiwan 10617, R.O.C.

Contributed by the Applied Mechanics Division of The American Society of Mechanical Engineers for publication in the ASME Journal of Applied Mechanics. Manuscript received by the ASME Applied Mechanics Division, Dec. 18, 1998; final revision, May 4, 1999. Associate Technical Editor: N. C. Perkins.

head-suspensions. In this note we study critical speed resonance in a space-fixed frame with emphasis on the effects of space-fixed damping on the stability of steady-state deflections. In the present formulation the forcing terms are time-invariant and no perturbation techniques are needed.

Equations of Motion

The dimensionless equations of motion of a disk spinning with constant speed Ω with respect to a space-fixed frame (r, θ) can be written as

$$w_{,tt} + 2\Omega w_{,t\theta} + \Omega^2 w_{,\theta\theta} + c_f w_{,t} + \nabla^4 w - r^{-1}(\sigma_r r w_{,r})_{,r} - r^{-2}\sigma_\theta w_{,\theta\theta} = w_{,rr}(r^{-1}\phi_{,r} + r^{-2}\phi_{,\theta\theta}) + (r^{-1}w_{,r} + r^{-2}w_{,\theta\theta})\phi_{,rr} - 2(r^{-1}w_{,\theta})_{,r}(r^{-1}\phi_{,\theta})_{,r} + q(r, \theta) \quad (1)$$

$$\nabla^4\phi = -\epsilon[w_{,rr}(r^{-1}w_{,r} + r^{-2}w_{,\theta\theta}) + 2r^{-3}w_{,r\theta}w_{,\theta} - r^{-2}(w_{,r\theta})^2 - r^{-4}(w_{,\theta})^2]. \quad (2)$$

w and ϕ are transverse displacement and stress function, respectively. The relations between dimensionless quantities and physical quantities (with asterisks) are

$$t = \frac{t^*}{b^2}\sqrt{\frac{D}{\rho h}}, \quad \Omega = \Omega^* b^2\sqrt{\frac{\rho h}{D}}, \quad r = \frac{r^*}{b},$$

$$w = w^*\sqrt{\frac{b}{h^3}}, \quad \phi = \phi^*\frac{h}{D}$$

$$q = q^*\sqrt{\frac{b^9}{D^2h^3}}, \quad c_f = c_f^*\frac{b^2}{\sqrt{\rho h D}}, \quad \epsilon = 12(1-\nu^2)\frac{h}{b}, \quad \eta = \frac{a}{b}.$$

The parameters ρ, h, E, ν, and D are the mass density, thickness, Young's modulus, Poisson ratio, and flexural rigidity of the disk, respectively. c_f^* represents a space-fixed homogeneous damping. $q^*(r^*, \theta)$ is the space-fixed time-invariant loading. The disk is assumed to be "partially clamped" at the inner radius $r^* = a$, and is free at the outer radius $r^* = b$ (Benson and Bogy, 1978). σ_r and σ_θ in Eq. (1) are dimensionless stresses due to centrifugal effect. In the special case when $\epsilon = 0$, the solution ϕ in Eq. (2) is identically zero, and as a consequence Eq. (1) reduces to

$$w_{,tt} + 2\Omega w_{,t\theta} + \Omega^2 w_{,\theta\theta} + c_f w_{,t} + \nabla^4 w - r^{-1}(\sigma_r r w_{,r})_{,r} - r^{-2}\sigma_\theta w_{,\theta\theta} = q. \quad (3)$$

Equation (3) is the conventional equation used in the literature without considering von Karman's effect. The natural frequency and the orthonormal eigenfunction of a freely spinning disk (i.e., $c_f = 0$, $q = 0$) are denoted by ω_{mn} and $w_{mn} = R_{mn}(r)e^{in\theta}$, respectively.

Steady-State Deflection Near Critical Speed

We assume that when the disk rotates near its critical speed Ω_c of mode w_{mn}, the solution w of Eqs. (1) and (2) can be approximated by a two-mode expansion,

$$w(r, \theta, t) = c_{mn}(t)w_{mn} + \bar{c}_{mn}(t)\bar{w}_{mn}. \quad (4)$$

Both $c_{mn}(t)$ and $w_{mn}(r, \theta)$ in Eq. (4) are complex functions. In order to solve ϕ in Eq. (2) we introduce a set of eigenfunctions ϕ_{mn} satisfying the following differential equation:

$$\nabla^4\phi_{mn} - \beta_{mn}^4\phi_{mn} = 0. \quad (5)$$

ϕ_{mn} satisfy the same boundary conditions as ϕ does. After expressing ϕ in terms of eigenfunctions series ϕ_{mn} and following Galerkin's procedure, we can discretize Eqs. (1) and (2) into

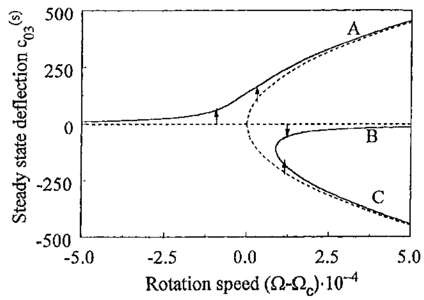

Fig. 1 Steady-state deflection $c_{03}^{(s)}$ near the critical speed

$$\ddot{c}_{mn} + (2in\Omega + c_f)\dot{c}_{mn} + \kappa_{mn}c_{mn} + \epsilon\gamma|c_{mn}|^2 c_{mn} - q_{mn} = 0 \quad (6)$$

where

$$q_{mn} = \int_{\theta=0}^{2\pi}\int_{r=\eta}^{1} q(r, \theta)R_{mn}(r)e^{-in\theta}rdrd\theta \quad (7)$$

$$\kappa_{mn} = \omega_{mn}(\omega_{mn} + 2n\Omega). \quad (8)$$

Constant γ can be obtained via numerical integration involving eigenfunctions w_{mn} and ϕ_{mn}. It is noted that for a reflected wave the integer n is considered as positive, while the natural frequency ω_{mn} is considered as negative. Therefore κ_{mn} is positive in the subcritical speed range, and is negative in the supercritical speed range. $|c_{mn}|$ represents the absolute value of complex number c_{mn}. The steady-state solutions $c_{mn}^{(s)}$ satisfy the equation

$$\kappa_{mn}c_{mn}^{(s)} + \epsilon\gamma|c_{mn}^{(s)}|^2 c_{mn}^{(s)} - q_{mn} = 0. \quad (9)$$

It is noted that this cubic equation allows only real roots. In the special case of a freely spinning disk when $q_{mn} = 0$, there is one trivial steady-state solution $c_{mn}^{(s)} = 0$ in the subcritical speed range $\Omega < \Omega_c$. On the other hand, in the supercritical speed range $\Omega > \Omega_c$, there are three real roots, i.e., $c_{mn}^{(s)} = 0$ and $c_{mn}^{(s)} = \pm\sqrt{-\kappa_{mn}/\epsilon\gamma}$. The dashed lines in Fig. 1 represent the steady-state deflections $c_{03}^{(s)}$ of a disk with clamping ratio $\eta = 0.5$ and Poisson ratio $\nu = 0.27$. The critical speed Ω_c of mode w_{03} is 8.75. The dimensionless thickness ϵ is taken to be 10^{-6} and the constant γ is calculated as 0.393.

In the case of a loaded disk with $q_{mn} > 0$, we can show that there is a modified critical speed $\Omega_c^* > \Omega_c$,

$$\Omega_c^* = \Omega_c + \frac{3}{2n^2\Omega_c}\left(\frac{\epsilon\gamma q_{mn}^2}{4}\right)^{1/3}. \quad (10)$$

When $\Omega < \Omega_c^*$ there is only one positive real root. On the other hand, there are three distinct real roots as $\Omega > \Omega_c^*$. The solid lines in Fig. 1 represent the steady-state solution $c_{03}^{(s)}$ when $q_{03} = 1$. The deflection A is always in the same direction as the applied load, while the deflections B and C are in the opposite direction. The small arrows in Fig. 1 indicate the deflection change from freely spinning disk to loaded disk.

Stability Analysis of Steady-State Solutions

In order to investigate the stability of the steady-state solutions, we express the solution c_{mn} in Eq. (6) as

$$c_{mn}(t) = c_{mn}^{(s)} + \hat{c}(t). \quad (11)$$

After substituting Eq. (11) into Eq. (6), using Eq. (9) and linearizing with respect to $\hat{c}$, we obtain the following equation:

$$\ddot{\hat{c}} + (2in\Omega + c_f)\dot{\hat{c}} + \kappa_{mn}\hat{c} + \epsilon\gamma(c_{mn}^{(s)})^2(2\hat{c} + \bar{\hat{c}}) = 0. \quad (12)$$

The eigenvalue λ of Eq. (12) can be obtained by solving the following quartic equation:

$$\lambda^4 + 2c_f\lambda^3 + [2\kappa_{mn} + 4\epsilon\gamma(c_{mn}^{(s)})^2 + c_f^2 + 4n^2\Omega^2]\lambda^2 + 2c_f[\kappa_{mn} + 2\epsilon\gamma(c_{mn}^{(s)})^2]\lambda + [\kappa_{mn} + 3\epsilon\gamma(c_{mn}^{(s)})^2][\kappa_{mn} + \epsilon\gamma(c_{mn}^{(s)})^2] = 0. \quad (13)$$

The steady-state solution is unstable when the real part of any of the four eigenvalues λ's is positive.

First of all we consider the deflections of the freely spinning disk with $c_f = 0$. For the trivial deflection $c_{mn}^{(s)} = 0$, the square of the eigenvalues solved from Eq. (13) are $\lambda^2 = -\omega_{mn}^2$ and $-(\omega_{mn} + 2n\Omega)^2$. For the nontrivial solutions $c_{mn}^{(s)} = \pm\sqrt{-\kappa_{mn}/\epsilon\gamma}$, $\lambda^2 = 0$ and $2\kappa_{mn} - 4n^2\Omega^2$. Therefore, the steady-state solutions of a freely spinning disk are neutrally stable to the first order of the stability analysis.

For the case of a loaded disk, it is difficult to express λ^2 in terms of physical parameters explicitly. However, we can study how λ^2 varies as q_{mn} increases from zero by differentiating Eq. (13) with respect to q_{mn} to obtain the first-order derivative $[\partial(\lambda^2)/\partial q_{mn}]|q_{mn=0}$. For the trivial solution $c_{mn}^{(s)} = 0$, we can show that the derivatives for $\lambda^2 = -\omega_{mn}^2$ and $-(\omega_{mn} + 2n\Omega)^2$ are zero. Therefore, deflection B remains neutrally stable when the space-fixed load is present.

For the nontrivial deflections $c_{mn}^{(s)} = \pm\sqrt{-\kappa_{mn}/\epsilon\gamma}$ in the supercritical speed range, the derivative for $\lambda^2 = 0$ is

$$\left.\frac{\partial(\lambda^2)}{\partial q_{mn}}\right|_{q_{mn}=0,\lambda^2=0} = \mp\frac{1}{2n^2\Omega^2 - \kappa_{mn}}\sqrt{\frac{-\kappa_{mn}}{\epsilon\gamma}}. \quad (14)$$

From Eq. (14) we can predict that λ^2 is negative for deflection A, and positive for deflection C. As a consequence, the steady-state deflection C of the loaded disk is unstable, and deflection A remains neutrally stable.

Space-Fixed Damping Effects

We next study the behavior of the eigenvalues when space-fixed damping is present. To do so, we differentiate Eq. (13) with respect to c_f and calculate the derivative at $c_f = 0$ and $q_{mn} = 0$. For the trivial solution $c_{mn}^{(s)} = 0$ the derivative of eigenvalue $\pm\omega_{mn}$ is

$$\left.\frac{\partial\lambda}{\partial c_f}\right|_{c_f=0,\lambda=\pm i\omega_{mn}} = \frac{-\omega_{mn}}{4n\Omega}. \quad (15)$$

In the supercritical speed range, the right-hand side of Eq. (15) is positive real. We therefore conclude that deflection B of the loaded disk is unstable in the presence of c_f.

For the negative deflection of the freely spinning disk, we first observe that c_f has no effect on the degenerate eigenvalues $\lambda = 0$. However, we have shown in the preceding section that applied load tends to drive one of these two degenerate eigenvalues to positive real for deflection C. Therefore, we conclude that deflection C of the loaded disk is also unstable when external damping c_f is present.

For the positive deflection of the freely spinning disk, applied load tends to drive the degenerate eigenvalues $\lambda = 0$ to purely imaginary, while c_f has no effect on these two eigenvalues. Therefore, deflection A is neutrally stable to the first order of the stability analysis. However, if we approximate λ of the undamped loaded disk by Eq. (14), then we obtain an estimate of the eigenvalue change of the loaded disk as

$$\left.\frac{\partial\lambda}{\partial c_f}\right|_{c_f=0} = \frac{\kappa_{mn}\sqrt{\epsilon\gamma}(2n^2\Omega^2 - \kappa_{mn}) - q_{mn}\sqrt{-\kappa_{mn}}}{2\sqrt{\epsilon\gamma}\,(2n^2\Omega^2 - \kappa_{mn})^2 - 2q_{mn}\sqrt{-\kappa_{mn}}}. \quad (16)$$

The right-hand side of Eq. (16) is negative for small q_{mn}. Therefore, c_f drives the eigenvalues from 0 to negative real. On the other hand, the derivative of the eigenvalues $\lambda = \pm i\sqrt{4n^2\Omega^2 - 2\kappa_{mn}}$ can be calculated as

$$\left.\frac{\partial\lambda}{\partial c_f}\right|_{c_f=0} = -1 + \frac{\kappa_{mn}}{4n^2\Omega^2 - 2\kappa_{mn}}. \quad (17)$$

The right-hand side of Eq. (17) is always negative. Therefore, we conclude that deflection A of the loaded disk is stabilized by the external damping.

References

Benson, R. C., and Bogy, D. B., 1978, "Deflection of a Very Flexible Spinning Disk Due to a Stationary Transverse Load," ASME Journal of Applied Mechanics, Vol. 45, pp. 636–642.

Nowinski, J. L., 1964, "Nonlinear Transverse Vibrations of a Spinning Disk," ASME Journal of Applied Mechanics, Vol. 31, pp. 72–78.

Raman, A., and Mote, Jr., C. D., 1999, "Non-linear Oscillations of Circular Plates Near a Critical Speed Resonance," *International Journal of Non-Linear Mechanics*, Vol. 34, pp. 139–157.

Tobias, S. A., and Arnold, R. N., 1957, "The Influence of Dynamical Imperfection on the Vibration of Rotating Disks," *Proceedings of the Institution of Mechanical Engineers*, Vol. 171, pp. 669–690.

Maximizing the Natural Frequencies and Transverse Stiffness of Centrally Clamped, Circular Disks by Thickening the Clamped Part of the Disk

A. A. Renshaw[1]

The natural frequencies and transverse stiffness of centrally clamped, circular disks are computed taking into account the flexibility of the central clamp and the thickness of the clamped part of the disk. When compared to experimental vibration data, these predictions are more accurate than the traditional, perfect clamping predictions, particularly for zero and one-nodal-diameter vibration modes. The reduction in natural frequency or transverse stiffness caused by clamping flexibility can be mitigated either by increasing the clamping stiffness or by increasing the hub thickness, defined here as the thickness of the disk sandwiched by the central clamp. A design study of these two alternatives for both stationary and rotating disks shows that increasing the hub thickness is often a more attractive design alternative.

1 Introduction

For the past decade, an interesting, industrial circular saw design has existed in which the hub thickness of the saw, defined here as the thickness of the part of the saw that is sandwiched between the thick clamping collars, is two to four times thicker than the exposed part of the saw (Bird, 1990). The origins of this design are unclear, although they may lie in the designs of unclamped, "free-floating" circular saws (Mote, 1977; Renshaw and Mote, 1996). The inventor of the design claims that increased hub thickness raises the critical speed of the saw *even for centrally clamped saws.* What is interesting about this claim is that the hub thickness is irrelevant in the traditional model of a centrally clamped saw.

[1] Department of Mechanical Engineering, Columbia University, M/C 4703, New York, NY 10027. Mem. ASME.

Contributed by the Applied Mechanics Division of The American Society of Mechanical Engineers for publication in the ASME Journal of Applied Mechanics. Manuscript received by the ASME Applied Mechanics Division, Feb. 10, 1999; final revision, May 4, 1999. Associate Technical Editor: N. C. Perkins.